

One-step electrochemical synthesis of graphene oxide-TiO₂ nanotubes for improved visible light activity

IMRAN ALI, SEU-RUN KIM, KYUNGMIN PARK, AND JONG-OH KIM*

Department of Civil and Environmental Engineering, Hanyang University, 222 Wangsimni-ro, Seongdong-gu, Seoul 04763, South Korea

*jk120@hanyang.ac.kr

Abstract: Graphene oxide (GO)-TiO₂ nanotubes (TNTs) were synthesized by one-step anodization. An as-prepared photocatalyst was characterized by FE-SEM, XRD, AES, PL, and UV-Vis DRS. To determine the effect of synthesis conditions on organics degradation, we prepared the catalyst with different GO concentrations, anodization voltages, and times. Optimum synthesis conditions were GO concentration 0.25 g L⁻¹ and anodization at 48 V for 2 h. Compared with TNTs, GO-TNTs showed a 3.6-fold increase in photocatalytic efficiency under visible light. Recycling was performed to investigate the stability of a GO-TNT catalyst. GO-TNTs is favorable for the separation of charges (e⁻/h⁺), promotion of the formation of OH[•], h⁺, and superoxides, which degrade organics.

© 2017 Optical Society of America

OCIS codes: (160.0160) Materials; (160.4236) Nanomaterials; (160.6000) Semiconductor materials.

References and links

1. M. Ehrampoosh, G. Moussavi, M. Ghaneian, S. Rahimi, and M. Ahmadian, "Removal of methylene blue dye from textile simulated sample using tubular reactor and TiO₂/UV-C photocatalytic process," *J. Environ. Health Sci. Eng.* **8**, 34–40 (2011).
2. E. Forgacs, T. Cserháti, and G. Oros, "Removal of synthetic dyes from wastewaters: a review," *Environ. Int.* **30**(7), 953–971 (2004).
3. Y. Wei, A. Ding, L. Dong, Y. Tang, F. Yu, and X. Dong, "Characterisation and coagulation performance of an inorganic coagulant—poly-magnesium-silicate-chloride in treatment of simulated dyeing wastewater," *Colloids Surf. A Physicochem. Eng. Asp.* **470**, 137–141 (2015).
4. P. Nuengmatcha, S. Chanthai, R. Mahachai, and W.-C. Oh, "Sonocatalytic performance of ZnO/graphene/TiO₂ nanocomposite for degradation of dye pollutants (methylene blue, texbrite BAC-L, texbrite BBU-L and texbrite NFW-L) under ultrasonic irradiation," *Dyes Pigments* **134**, 487–497 (2016).
5. S. Sathian, M. Rajasimman, C. Rathnasabapathy, and C. Karthikeyan, "Performance evaluation of SBR for the treatment of dyeing wastewater by simultaneous biological and adsorption processes," *J. Water Process Eng.* **4**, 82–90 (2014).
6. W.-Y. Choi, Y.-W. Lee, and J.-O. Kim, "Factors affecting preparation of photocatalytic TiO₂ metal membrane with reactive nano-structured tubes," *Desalin. Water Treat.* **34**(1-3), 229–233 (2011).
7. B. Wang, H. Qi, H. Wang, Y. Cui, J. Zhao, J. Guo, Y. Cui, Y. Liu, K. Yi, and J. Shao, "Morphology, structure and optical properties in TiO₂ nanostructured films annealed at various temperatures," *Opt. Mater. Express* **5**(6), 1410–1418 (2015).
8. M. S. Park, S.-J. Lee, S.-J. Sung, and D.-H. Kim, "Double-layered TiO₂ photoelectrode with particulate structure prepared by one-step soaking method," *Opt. Mater. Express* **4**(11), 2401–2408 (2014).
9. D. He, Y. Hu, J. Tao, X. Zheng, H. Liu, G. Jing, H. Lu, H. Guan, J. Yu, J. Zhang, J. Tang, Y. Luo, and Z. Chen, "Micro fiber with cladding of titanium dioxide (TiO₂) nanoparticles and its violet light sensing," *Opt. Mater. Express* **7**(1), 264–272 (2017).
10. S. Karlsson, L. G. Bäck, P. Kidkhunthod, K. Lundstedt, and L. Wondraczek, "Effect of TiO₂ on optical properties of glasses in the soda-lime-silicate system," *Opt. Mater. Express* **6**(4), 1198–1216 (2016).
11. A. Ziełńska-Jurek and J. Hupka, "Preparation and characterization of Pt/Pd-modified titanium dioxide nanoparticles for visible light irradiation," *Catal. Today* **230**, 181–187 (2014).
12. S.-P. Kim and J.-O. Kim, "Fabrication, characterization and photocatalytic performance of Fe-doped TiO₂ nanotube composite for efficient degradation of water pollutants," *Desalin. Water Treat.*, 1–7 (2015).
13. Y. Niu, M. Xing, J. Zhang, and B. Tian, "Visible light activated sulfur and iron co-doped TiO₂ photocatalyst for the photocatalytic degradation of phenol," *Catal. Today* **201**, 159–166 (2013).
14. S. Li, Z. Ma, J. Zhang, Y. Wu, and Y. Gong, "A comparative study of photocatalytic degradation of phenol of TiO₂ and ZnO in the presence of manganese dioxides," *Catal. Today* **139**(1-2), 109–112 (2008).

15. M.-Q. Yang, N. Zhang, and Y.-J. Xu, "Synthesis of fullerene-, carbon nanotube-, and graphene-TiO₂ nanocomposite photocatalysts for selective oxidation: a comparative study," *ACS Appl. Mater. Interfaces* **5**(3), 1156–1164 (2013).
16. N. Zhang, M.-Q. Yang, S. Liu, Y. Sun, and Y.-J. Xu, "Waltzing with the versatile platform of graphene to synthesize composite photocatalysts," *Chem. Rev.* **115**(18), 10307–10377 (2015).
17. Q. Quan, X. Lin, N. Zhang, and Y.-J. Xu, "Graphene and its derivatives as versatile templates for materials synthesis and functional applications," *Nanoscale* **9**(7), 2398–2416 (2017).
18. A. K. Geim and K. S. Novoselov, "The rise of graphene," *Nat. Mater.* **6**(3), 183–191 (2007).
19. Q. Xiang, J. Yu, and M. Jaroniec, "Graphene-based semiconductor photocatalysts," *Chem. Soc. Rev.* **41**(2), 782–796 (2012).
20. Y. Zhang, Z.-R. Tang, X. Fu, and Y.-J. Xu, "TiO₂-graphene nanocomposites for gas-phase photocatalytic degradation of volatile aromatic pollutant: is TiO₂-graphene truly different from other TiO₂-carbon composite materials?" *ACS Nano* **4**(12), 7303–7314 (2010).
21. M.-Q. Yang, C. Han, N. Zhang, and Y.-J. Xu, "Precursor chemistry matters in boosting photoredox activity of graphene/semiconductor composites," *Nanoscale* **7**(43), 18062–18070 (2015).
22. W.-Y. Choi, J. Chung, C.-H. Cho, and J.-O. Kim, "Fabrication and photocatalytic activity of a novel nanostructured TiO₂ metal membrane," *Desalination* **279**(1-3), 359–366 (2011).
23. S. Zhu, X. Liu, J. Lin, and X. Chen, "Low temperature transferring of anodized TiO₂ nanotube-array onto a flexible substrate for dye-sensitized solar cells," *Opt. Mater. Express* **5**(12), 2754–2760 (2015).
24. P. Song, X. Zhang, M. Sun, X. Cui, and Y. Lin, "Graphene oxide modified TiO₂ nanotube arrays: enhanced visible light photoelectrochemical properties," *Nanoscale* **4**(5), 1800–1804 (2012).
25. C. Zhai, M. Zhu, Y. Lu, F. Ren, C. Wang, Y. Du, and P. Yang, "Reduced graphene oxide modified highly ordered TiO₂ nanotube arrays photoelectrode with enhanced photoelectrocatalytic performance under visible-light irradiation," *Phys. Chem. Chem. Phys.* **16**(28), 14800–14807 (2014).
26. F. Gobal and M. Faraji, "Electrochemical synthesis of reduced graphene oxide/ TiO₂ nanotubes/Ti for high-performance supercapacitors," *Ionics* **21**(2), 525–531 (2015).
27. N. Lingappan, Y.-S. Gal, and K. T. Lim, "Synthesis of reduced graphene oxide/polypyrrole conductive composites," *Mol. Cryst. Liquid Cryst.* **585**(1), 60–66 (2013).
28. S. El-Kacemi, H. Zazou, N. Oturan, M. Dietze, M. Hamdani, M. Es-Souni, and M. A. Oturan, "Nanostructured ZnO-TiO₂ thin film oxide as anode material in electrooxidation of organic pollutants. Application to the removal of dye Amido black 10B from water," *Environ. Sci. Pollut. Res.* **24**, 1–8 (2016).
29. G. S. Thien, F. S. Omar, N. I. S. A. Blya, W. S. Chiu, H. N. Lim, R. Yousefi, F.-J. Sheini, and N. M. Huang, "Improved synthesis of reduced graphene oxide-titanium dioxide composite with highly exposed 001 facets and its photoelectrochemical response," *Int. J. Photoenergy* **2014**, 1–9 (2014).
30. Y. Lai, L. Sun, Y. Chen, H. Zhuang, C. Lin, and J. W. Chin, "Effects of the structure of TiO₂ nanotube array on Ti substrate on its photocatalytic activity," *J. Electrochem. Soc.* **153**(7), D123–D127 (2006).
31. F. Duo, Y. Wang, C. Fan, X. Mao, X. Zhang, Y. Wang, and J. Liu, "Low temperature one-step synthesis of rutile TiO₂/BiOCl composites with enhanced photocatalytic activity," *Mater. Charact.* **99**, 8–16 (2015).
32. H. Li, Z. Xia, J. Chen, L. Lei, and J. Xing, "Constructing ternary CdS/reduced graphene oxide/ TiO₂ nanotube arrays hybrids for enhanced visible-light-driven photoelectrochemical and photocatalytic activity," *Appl. Catal. B* **168**, 105–113 (2015).
33. V. R. Posa, V. Annavaram, J. R. Koduru, P. Bobbala, and A. R. Somala, "Preparation of graphene- TiO₂ nanocomposite and photocatalytic degradation of Rhodamine-B under solar light irradiation," *J. Exp. Nanosci.* **11**(9), 722–736 (2016).
34. K. Zhou, Y. Zhu, X. Yang, X. Jiang, and C. Li, "Preparation of graphene- TiO₂ composites with enhanced photocatalytic activity," *New J. Chem.* **35**(2), 353–359 (2011).
35. N. Khalid, E. Ahmed, Z. Hong, L. Sana, and M. Ahmed, "Enhanced photocatalytic activity of graphene- TiO₂ composite under visible light irradiation," *Curr. Appl. Phys.* **13**(4), 659–663 (2013).
36. N. Raghavan, S. Thangavel, and G. Venugopal, "Enhanced photocatalytic degradation of methylene blue by reduced graphene-oxide/titanium dioxide/zinc oxide ternary nanocomposites," *Mater. Sci. Semicond. Process.* **30**, 321–329 (2015).

1. Introduction

The paper, plastic, dyeing, and textile industries consume color and a large volume of water for dyeing their products. Additionally, these processes produce wastewater that contains dyestuffs, which have a detrimental effect on the environment [1]. Once dyes enter wastewater, they become more stable, and the complex aromatic structures of these materials may interfere with their natural biodegradation processes [2]. Therefore, these dye contaminants must be removed from wastewater before they are released into the environment.

In order to lower the levels of these pollutants in the effluent to an acceptable level, it is necessary to develop an efficient and inexpensive method. Several methods have been applied

for the treatment of dye contaminants including chemical precipitation [3], membrane filtration [4], and adsorption [5]. However, in these treatment methods, a further separation technique is required to dispose of the large amounts of residual sludge that they produce.

In recent years, photocatalytic degradation of organic contaminants using semiconductor-based nanomaterials has greatly advanced [6, 7]. TiO_2 plays a leading role in photocatalysis because of its availability, stability, non-toxicity, chemical inertness, and efficacy in the oxidation of various organic molecules [8, 9]. TiO_2 produces hydroxyl (OH) radicals that have been used to decompose organic contaminants. However, TiO_2 shows decreased efficiency under visible light because its band gap energy (~ 3.2 eV [10]) is activated by ultraviolet (UV) light; solar light is made up of only 5% UV light [11]. Furthermore, TiO_2 exhibits high recombination of electrons (e^-) and holes (h^+). To overcome these drawbacks, different strategies have been used such as metal deposition [12], non-metal doping [13], and coupling with other semiconductors [14].

Recently, research into visible-response photocatalysts has become popular; these investigations have generally focused on materials such as carbon, fullerene, and graphene [15–17]. Graphene has attracted much attention due to its mechanical, electronic, and thermal properties [18]. Furthermore, graphene oxide (GO) has been shown to increase the efficiency of TiO_2 under visible light. It increases the adsorption of organics on TiO_2 surfaces and reduces the recombination of e^- and h^+ [19–21].

Anodization is a useful method for modifying TiO_2 surfaces and for achieving a nanotubular structure [22, 23]. Many researchers have used GO as a modification material for anodized TiO_2 nanotubes (TNTs). This has been completed with a variety of GO coupling strategies such as the simple dipping method [24], vapor thermal treatment [25], and electrochemical deposition [26]. These TNT alterations were achieved using a two-step process: anodization of the TNTs followed by GO coupling. To improve this two-step experimental method, we proposed a one-step synthesis process. This reported synthesis process is highly practical, consumes less energy, and requires a relatively short time for synthesis.

In this study, we synthesized an enhanced visible-light GO-TNTs photocatalyst with a new one-step anodization method. We determined the effects of different GO concentrations, anodization voltages, and anodization times on the degradation of organics. We also found the optimum synthesis conditions necessary to produce a photocatalyst with a strong visible-light response. Recycling of GO-TNTs was also carried out in order to investigate the stability of the catalyst. The synergistic effects of GO coupling were also discussed with the proposed organics removal mechanism.

2. Material and methods

2.1 Chemicals

Graphite powder (99.99%) and Ti foil (99.5%, 2×5 cm², and a thickness of 0.25 mm) were provided by Alfa Aesar, Korea. The other chemicals used in this study were methylene blue dye (MB) ($\text{C}_{16}\text{H}_{18}\text{ClN}_3\text{S}$, 95.0%, Showa, Japan), ethylene glycol ($\text{C}_2\text{H}_6\text{O}_2$, 94.5%, Daejung, Korea), potassium permanganate (KMnO_4 , 99.3%, Duksan, Korea), sulfuric acid (H_2SO_4 , 98.1%, Daejung, Korea), ammonium fluoride (NH_4F , 97.0%, Junsei, Japan), hydrochloric acid (HCl , >35%, Daejung, Korea), and sodium nitrate (NaNO_3 , >99.0%, Daejung, Korea). All of these chemicals were of analytical grade and were used without further purification.

2.2 Synthesis of catalyst

2.2.1 Synthesis of graphene oxide

GO was synthesized by a modified Hummer's method [27]. First, 1 g of graphite powder, 0.5 g of sodium nitrate, and 25 mL of sulfuric acid were mixed. Then, 3 g of potassium permanganate was added and mixed for 12 h at 35 °C. The obtained brown-colored GO

solution was washed five times with deionized (DI) water and a 1 M hydrochloric acid before being dried at 60 °C.

2.2.2 Synthesis of GO-TNTs

For synthesis of one-step GO-TNT first, to remove impurities, Ti foil was sonicated in acetone, ethanol, and DI water (for 10 min each) and then dried with N₂ gas. The electrolyte solution consisted of ethylene glycol (EG):DI water (94:5 wt%), ammonium fluoride (1 wt%), and different concentrations of GO (0.125 - 1.0 g L⁻¹). Platinum was used as the cathode, and a distance of 2 cm was maintained between the two electrodes. Anodization was achieved at different voltages (40 - 65 V) and different anodization times (1.5 - 3.5 h), as shown in Table 1. Anodization was performed using an N6702A power supply (Agilent Technologies, Spain). After anodization, the Ti foil was washed with DI water and dried with N₂ gas. To improve the anatase crystalline structure of TiO₂, annealing was performed at 550 °C for 1.5 h in a furnace.

For synthesis of two-step GO-TNT, firstly TNT was synthesized using electrolyte EG:DI water (94:5 wt%) with ammonium fluoride (1 wt%). Anodization was performed at 48 V for 2 h, then annealing at 550 °C for 1.5 h. In second step GO was attached through electrochemical anodization using GO concentration of 0.25 g L⁻¹ and anodization at 48 V for 1 min, then dried at 60 °C for 12 h.

Table 1. Synthesis conditions of the one-step GO-TNTs catalyst with different GO concentrations, anodization voltages, and anodization times.

Order	GO concentration (g L ⁻¹)	Anodization time (h)	Anodization voltage (V)
1	0.125	2.0	48
2	0.25	2.0	48
3	0.50	2.0	48
4	0.75	2.0	48
5	1.00	2.0	48
6	0.25	1.5	48
7	0.25	2.5	48
8	0.25	3.0	48
9	0.25	3.5	48
10	0.25	2.0	40
11	0.25	2.0	55
12	0.25	2.0	60
13	0.25	2.0	65

2.3 Characterization

The surface structure of the GO-TNTs catalyst was analyzed using field emission scanning electron microscopy (FE-SEM, Sigma, Carl Zeiss Co., Germany). The crystalline material phase was identified by X-ray diffraction (XRD, D8-Advance, Bruker-AXS Co., Germany). The atomic composition and surface analysis of the catalyst were measured by Auger electron spectroscopy (AES 700, PHI 700 xi). The excited state of the semiconductor was determined using photoluminescence spectroscopy (Micro Confocal PL, Mono Ra 750i) using excitation wavelength of 325 nm, and the emission was observed from 300 to 800 nm in a single scan mode with He-Cd laser. The band gap energy was identified using UV-Vis diffuse reflectance spectroscopy (Lambda 650S, Perkin Elmer).

2.4 Photocatalytic experiments

The photocatalytic degradation performance of the visible-light GO-TNTs catalyst was used to examine the degradation of MB dye. A 35 mL MB solution with an initial concentration of 5 mg L^{-1} was used in a laboratory-scale reactor. The glass reactor having inner diameter of 9 cm and height of 5 cm, with visible lamps mounted above the MB solution. The Ti catalyst film size was $2 \times 5 \text{ cm}^2$. Visible-light photocatalytic activity was achieved using a fluorescent lamp (32 W, $\lambda = 400\text{-}700 \text{ nm}$, Philips Co., Netherlands) at room temperature. The fluorescent lamp luminous efficacy was up to 90 lm w^{-1} and we have used UV cut off filter to remove wavelength $< 420 \text{ nm}$. The photoelectrocatalytic activity was tested at an external bias of 5 V. First, the experiment was performed in the dark for 20 min to achieve adsorption equilibrium. Later, visible light was supplied for 150 min. The quantity of MB degradation was measured using UV-Vis spectrophotometry (DR3900, HACH, USA) at a wavelength of 664 nm.

A reusability experiment was also carried out for the GO-TNTs catalyst to examine the stability of the visible-light catalyst. The experimental conditions were the same as those used for the photoelectrocatalytic process with an external bias of 5 V. After each cycle, the GO-TNTs catalyst was washed with DI water and dried in an oven at $70 \text{ }^\circ\text{C}$ for 1 h in order to remove any deposits and impurities from the catalyst surface.

3. Results and discussion

3.1 Characterization

3.1.1 FE-SEM and XRD

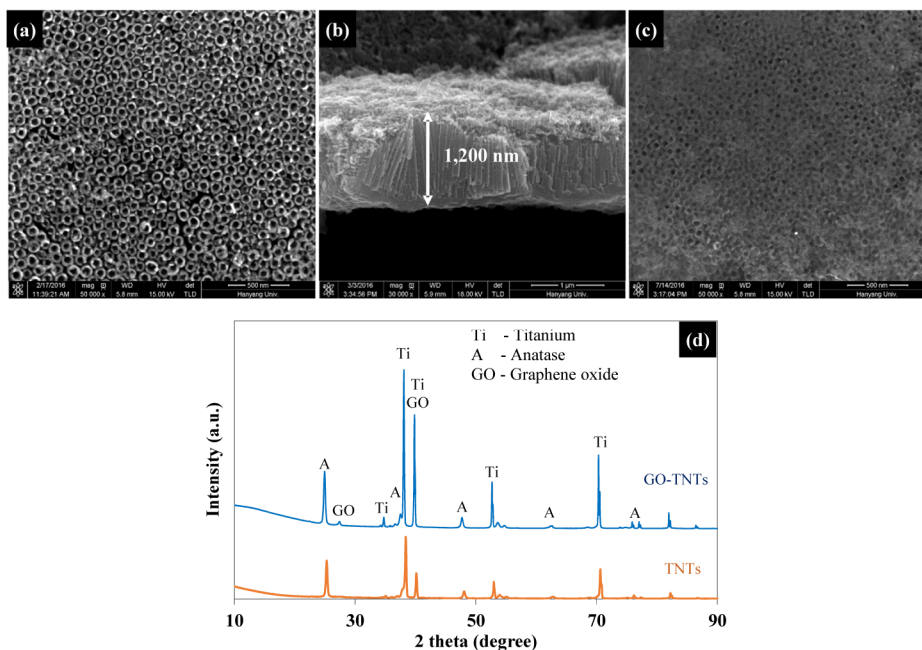


Fig. 1. FE-SEM images of: (a) TNTs, (b) cross view, and (c) GO-TNTs, (d) XRD patterns of TNTs and GO-TNTs.

Figures 1(a)-1(c) show FE-SEM images of the TNTs and one-step prepared GO-TNTs composite. Uniform and highly-oriented TiO_2 nanotubes were achieved by anodization. The TiO_2 nanotube diameter was about 50 nm, and the nanotube length was 1,200 nm, as shown in Figs. 1(a) and 1(b), respectively. The optimum photocatalytic degradation results were found at synthesis conditions of GO concentration 0.25 g L^{-1} , anodization voltage 48 V, and

anodization time 2 h and the FE-SEM is shown in Fig. 1(c). The FE-SEM image of GO-TNTs show that GO was well adhered to the TiO_2 surface and filled the interior of the nanotube surface. This is because nanotube formation and GO coupling occurred at the same time.

The XRD patterns of TNTs and one-step GO-TNTs composite are shown in Fig. 1(d). The TNT films were annealed at 550 °C for 1.5 h in order to obtain the anatase crystalline structure. The anatase TiO_2 diffraction peaks at 25.3°, 37.9°, 48.1°, and 55.0° correspond to the (101), (004), (200), and (105) planes, respectively [28]. The XRD spectrum of the GO-TNTs composite shows diffraction peaks of anatase and Ti phases of TNTs together with GO. Two GO peaks with low intensity were also observed at 26.3° and 41.1° overlapped with Ti peak [26].

3.1.2 Auger electron spectroscopy

The atomic composition and surface mapping of the one-step GO-TNTs prepared via our one-step fabrication process are shown in Fig. 2. GO, as carbon (C), appears as the dark regions in Fig. 2(a). The other elements of Ti and oxygen (O), can be seen in Figs. 2(b) and (c), respectively. Figure 2(d) shows the AES atomic compositions of the one-step GO-TNTs. The atomic compositions of C, O, and Ti were 5.8, 62.0, and 32.2%, respectively. From the AES results, it was confirmed that GO was successfully coupled with the anodized TNT surface.

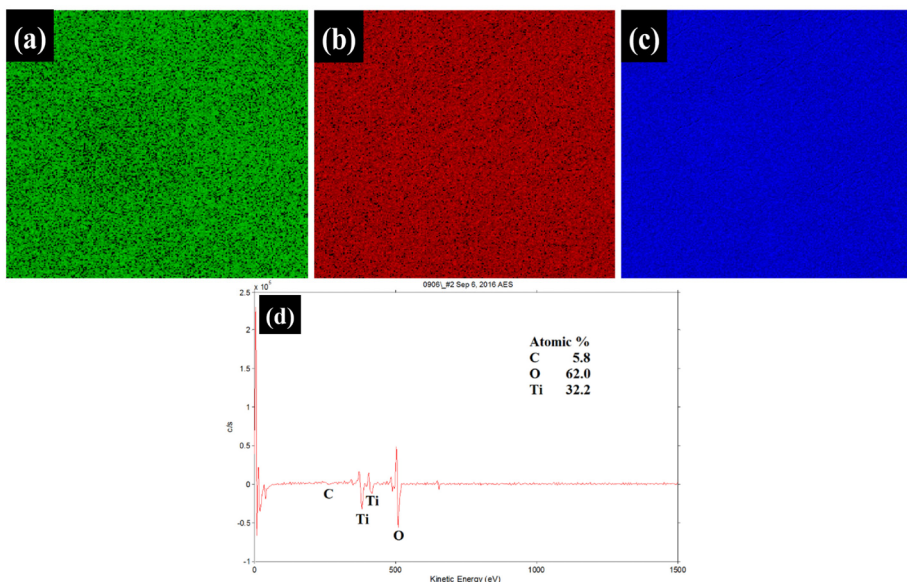


Fig. 2. AES analysis results of GO-TNTs: (a) carbon, (b) oxygen, (c) Ti, and (d) atomic composition.

3.1.3 Photoluminescence and UV-Vis diffuse reflectance spectra

The photoluminescence (PL) spectra of the TNTs and GO-TNTs one-step and two-step composites are shown in Fig. 3(a). The PL data indicate the excited state of the photocatalyst semiconducting material, which was affected by the recombination of photogenerated charges (e^- and h^+) [29]. Here, a lower PL intensity indicates better charge separation of e^- and h^+ . In Fig. 3(a), a low PL spectra intensity was observed for the GO-TNTs catalyst prepared with our one-step process than other catalysts. This was due to the fact that graphene acts as an electron transport material for TiO_2 to reduce recombination of e^- and h^+ . This increased the efficiency of the photocatalytic activity of the GO-TNTs composite under visible light.

Figure 3(b) shows the UV-Vis diffuse reflectance spectroscopy (DRS) results of TNTs and GO-TNTs one-step and two-step composites. Pure TNTs showed absorption in the UV-

light region at the band gap energy of anatase TiO₂ 3.18 eV. Alternatively, the GO-TNT one-step and two-step catalysts showed absorbance within the visible-light region with an approximate band gap energy of 2.87 eV and 2.89 eV, respectively. This result corresponds to the sub-band gap conditions of the TNTs [30]. Compared with pure TNTs, the absorption of the GO-TNTs catalyst in the visible-light region was increased due to the GO coupling. The band gap energy was calculated using Eq. (1):

$$E_g = \frac{hc}{\lambda} \quad (1)$$

Here, E_g is the band gap energy in eV, h is Plank's constant, c is the speed of light, and λ is the wavelength in nm.

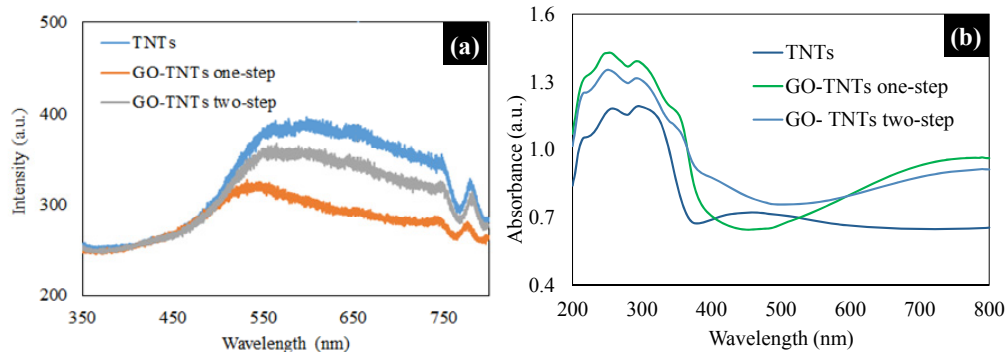


Fig. 3. TNT and GO-TNT one-step and two-step catalysts: (a) PL spectra and (b) UV-Vis DRS.

3.2 Photocatalytic degradation results

3.2.1 Effect of GO concentration on MB degradation

Figure 4 shows the effect of GO concentration (0.125 - 1.0 g L⁻¹) on the degradation of MB. Here, we fixed the anodization voltage at 48 V and the anodization time at 2 h. The photocatalytic MB degradation was 44, 57, 48, 45, and 41% at GO concentrations of 0.125, 0.25, 0.5, 0.75, and 1.0 g L⁻¹, respectively. We observed that the optimum GO concentration for MB degradation occurred at 0.25 g L⁻¹ under visible light. The photocatalytic results showed that MB degradation was increased with increasing GO concentration up to 0.25 g L⁻¹; at higher concentrations, the degradation performance decreased. The decrease in MB degradation above 0.25 g L⁻¹ was due to excess GO loading, which may have caused the formation of a dense layer of GO on the TiO₂ nanotube surface, thereby reducing the photocatalytic efficiency.

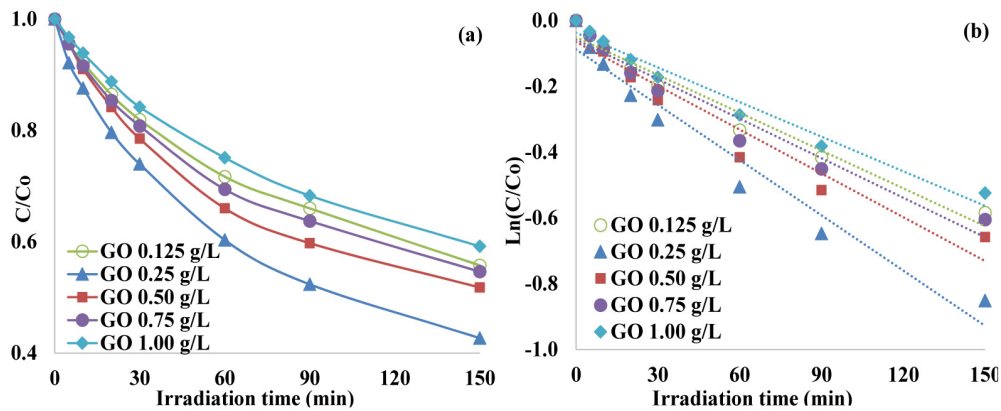


Fig. 4. Effect of GO concentration on MB degradation under visible light at a fixed anodization time of 2 h and an anodization voltage of 48 V: (a) C/C_0 and (b) $\ln(C/C_0)$.

3.2.2 Effect of anodization time on MB degradation

To determine the effect of anodization time on MB degradation, the photocatalytic activity was performed at different anodization times (1.5 - 3.5 h), as shown in Fig. 5. Here, we fixed the GO concentration at 0.25 g L^{-1} and the anodization voltage at 48 V. The photocatalytic MB degradation was 42, 57, 55, 53, and 35% at anodization times of 1.5, 2.0, 2.5, 3.0, and 3.5 h, respectively. We observed that the optimum anodization time for MB degradation was 2 h. The photodegradation results showed that the degradation rate of MB increased with increasing anodization times up to 2 h; for longer anodization times, the degradation rate was reduced. The reduction in MB degradation above 2 h was caused by the fact that longer anodization times can affect the TiO_2 nanotube length. This resulted in a reduction of the photocatalytic efficiency in the GO-TNT composite prepared with our one-step process.

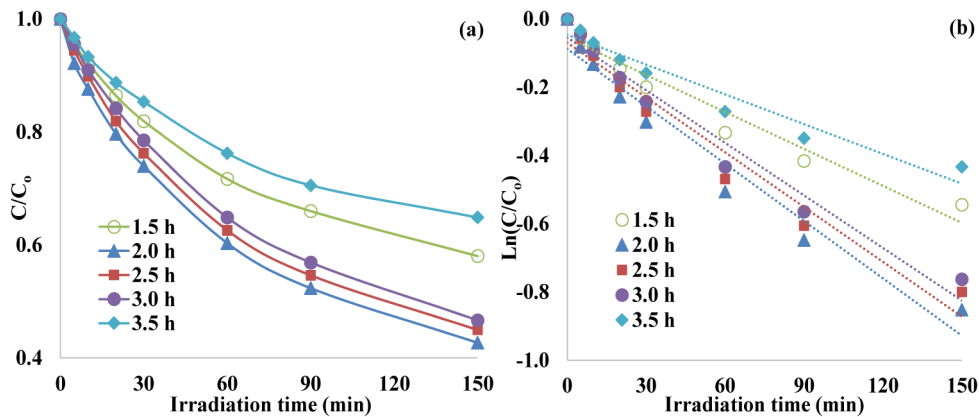


Fig. 5. Effect of anodization time on MB degradation under visible light at a fixed GO concentration of 0.25 g L^{-1} and an anodization voltage of 48 V: (a) C/C_0 and (b) $\ln(C/C_0)$.

3.2.3 Effect of anodization voltage on MB degradation

Figure 6 shows the effect of anodization voltage (40 - 65 V) on MB degradation. Here, we fixed the anodization time at 2 h and the GO concentration at 0.25 g L^{-1} . The photocatalytic MB degradation was 43, 57, 50, 31, and 23% at anodization voltages of 40, 48, 55, 60, and 65 V, respectively. We observed that the optimum anodization voltage for MB degradation was 48 V. The photocatalytic results showed that MB degradation increased with increasing anodization voltage up to 48 V; for higher anodization voltages, MB degradation decreased.

The decrease in MB degradation above 48 V was due to the excess anodization voltage, which can affect the TiO_2 nanotube diameter, thereby reducing the overall photocatalytic efficiency.

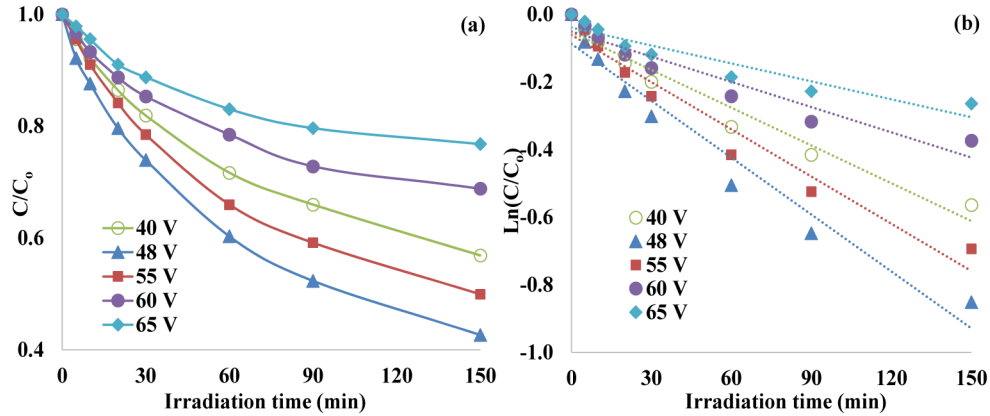


Fig. 6. Effect of anodization voltage on MB degradation under visible light at a fixed GO concentration of 0.25 g L^{-1} and an anodization time of 2 h: (a) C/C_0 and (b) $\ln(C/C_0)$.

3.2.4 Comparison of photocatalytic results

The comparison of the photocatalytic degradation of MB by TNTs and GO-TNTs one-step and two-step catalysts is shown in Fig. 7. Very little MB degradation was observed when the experiment was conducted using only catalyst or photolysis. This blank experiment confirmed that TiO_2 catalyst needs a light source to degrade organics [31]. The visible-light one-step GO-TNT composite showed a higher MB degradation rate compared with two-step GO-TNTs and pure TNTs. The MB degradation was 16, 57 and 41% by TNTs, GO-TNTs one-step and two-step, respectively. The GO-TNT composite prepared with our one-step process (optimum synthesis conditions: GO concentration of 0.25 g L^{-1} and anodization at 48 V for 2 h) showed a 3.6-fold increase in MB degradation compared to the pure TNTs.

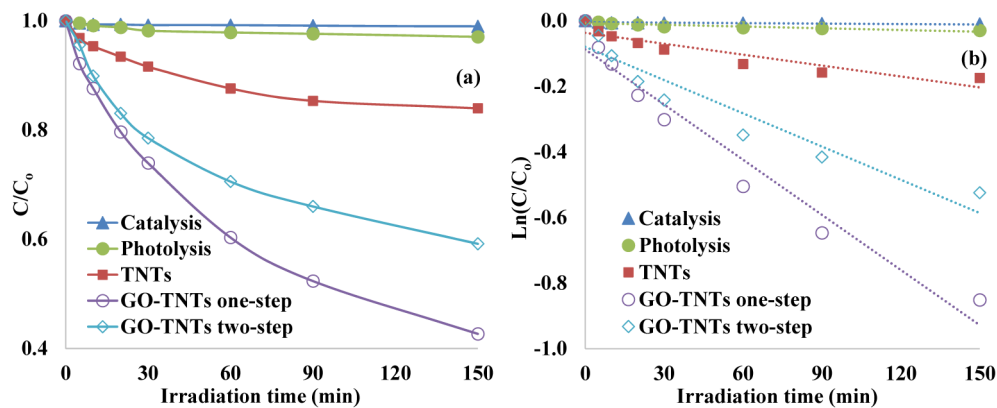


Fig. 7. Photocatalytic degradation of MB dye under visible light irradiation by TNTs and GO-TNTs one-step and two-step: (a) C/C_0 and (b) $\ln(C/C_0)$.

Improved visible-light photocatalytic degradation efficiency of GO-modified TNT composites was also observed in previous studies by Li et al. [32] and Song et al. [24]. They observed enhanced MB degradation of GO-modified TNTs under visible-light irradiation compared with pure TNTs. The reaction rate constant values (k) were calculated according to Eq. (2):

$$\ln \frac{C}{C_0} = -kt \quad (2)$$

Here, C is the MB concentration at a particular time, C_0 is the initial MB concentration, k is a pseudo first-order reaction rate constant in min^{-1} , and t is the light irradiation time in min. The summary of the reaction rate constant values and their associated R^2 values for TNTs and GO-TNTs is shown in Table 2. The photocatalytic activity of the one-step GO-TNT composite (optimum synthesis conditions: GO concentration of 0.25 g L^{-1} , anodization voltage of 48 V, and anodization time of 2 h) has a higher reaction rate constant value (0.0057 min^{-1}) than any of the other samples. This sample also showed a higher photocatalytic degradation activity (57%) for MB dye.

Here, higher visible-light photocatalytic activity of GO-TNTs was observed for the following reasons. GO coupling may reduce the band gap energy of the TiO_2 , which enhances the absorption of TNTs under visible light irradiation [24]. GO coupled on TiO_2 can trap photogenerated electrons, thereby reducing the recombination of charges e^- and h^+ . Also, the specific surface areas of GO-TNT composites are large, which helps the adsorption of organics onto the photocatalyst surface and provides more accessible active sites for the degradation of organics [32].

Table 2. Reaction rate constant values (k) and associated R^2 values for TNTs and GO-TNTs.

Sample	k (min^{-1})	R^2
Catalysis	0.0001	0.5499
Photolysis	0.0002	0.8209
TNTs	0.0012	0.8541
GO-TNTs 0.125 g L^{-1}	0.0039	0.9668
GO-TNTs 0.25 g L^{-1}	0.0057	0.9559
GO-TNTs 0.50 g L^{-1}	0.0044	0.9410
GO-TNTs 0.75 g L^{-1}	0.0040	0.9542
GO-TNTs 1.00 g L^{-1}	0.0035	0.9718
GO-TNTs 1.5 h	0.0036	0.9489
GO-TNTs 2.5 h	0.0053	0.9592
GO-TNTs 3.0 h	0.0051	0.9676
GO-TNTs 3.5 h	0.0029	0.9388
GO-TNTs 40 V	0.0038	0.9586
GO-TNTs 55 V	0.0046	0.9550
GO-TNTs 60 V	0.0025	0.9136
GO-TNTs 65 V	0.0018	0.8863
GO-TNTs two-step	0.0035	0.9021

3.2.5 Reusability investigation

A reusability investigation was performed to determine the stability of the visible-light GO-TNT catalyst (GO concentration of 0.25 g L^{-1} and anodization at 48 V for 2 h). The reusability experiment was carried out for five cycles, as shown in Fig. 8. The experimental conditions were the same as those used for the photocatalytic process. The degradation efficiency for the GO-TNT composite prepared with our one-step process was stable, even after four cycles. This catalyst was stable due to the fact that nanotube formation and GO coupling occurred at the same time.

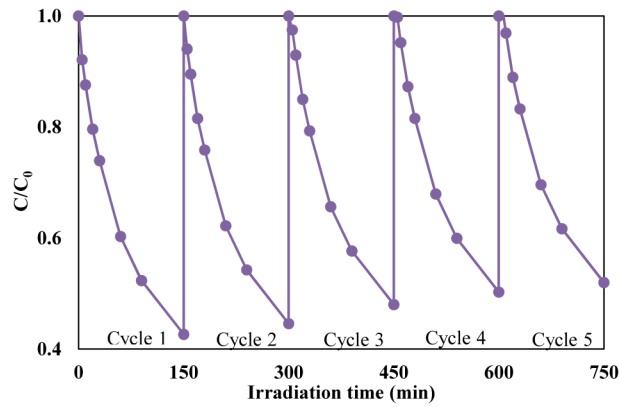
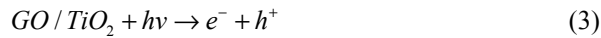


Fig. 8. Reusability investigation of GO-TNT catalyst under visible light.

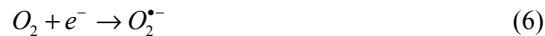
3.2.6 Photocatalysis mechanism of modified TiO₂

Here, we propose a possible photocatalysis mechanism for the GO-modified TiO₂, as shown in Fig. 9. This photocatalytic degradation mechanism contains these four steps: (1) the visible light irradiation on TiO₂ surface improved by the GO, (ii) the excitation of e⁻ from valance band (VB) to the conduction band (CB) of TiO₂, and leaving the h⁺ in VB, (iii) the e⁻ and h⁺ firstly reacts with H₂O, and (iv) then induced the degradation of organics [33].

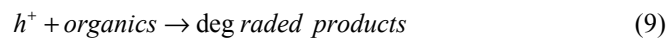
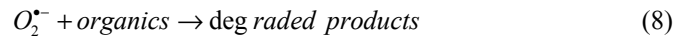
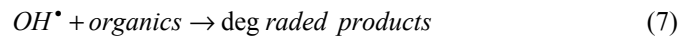
The organics degradation by the modified photocatalytic process can be explained by Eqs. (3-9). Initially, when exposed to visible-light irradiation, the GO-TiO₂ photocatalyst generates e⁻ and h⁺ [34]. The generated e⁻ from the CB of TiO₂ [35] leaving h⁺ in the VB of TiO₂.



The generated h⁺ on the TiO₂ surface reacts with water or hydroxide ions (OH⁻) to produce hydroxyl radicals (OH[•]), and the generated e⁻ reacts with O₂ to produce superoxides (O₂^{•-}).



OH[•], O₂^{•-}, and h⁺ degrade the organics into the oxidized products [36].



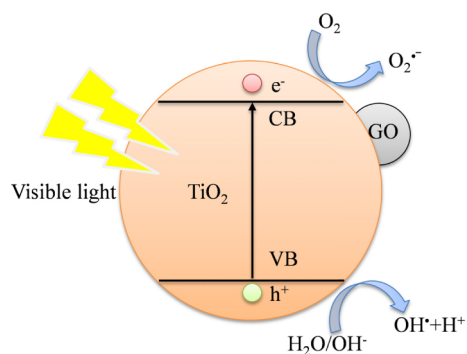


Fig. 9. Photocatalysis mechanism of GO-modified TiO₂.

4. Conclusions

An enhanced visible-light GO-TNT photocatalyst was successfully synthesized and confirmed by FE-SEM, XRD, AES, PL, and UV-Vis DRS analysis. The GO-TNT catalyst was prepared by a one-step anodization process. We determined the effect of GO concentration, anodization voltage, and anodization time on the degradation of organics. The optimum synthesis conditions were a GO concentration of 0.25 g L⁻¹ with an anodization voltage of 48 V and an anodization time of 2 h. This sample showed a high photocatalytic activity for organics degradation under visible light. The photocatalytic activity of the GO-TNT composite was 3.6 times higher than that of pure TNTs. Additionally, the recycling results indicated that the GO-TNT composite was stable for many cycles and showed efficient separation of charges (e⁻ and h⁺). The organics removal was due to the formation of OH radicals, h⁺, and superoxides. The observed increase in visible-light photocatalytic activity of the GO-TNT was caused by the GO coupling.

Funding

National Research Foundation of Korea (NRF) (NRF-2016R1A2A1A05005388).